MODELING P WAVE MULTIPATHING IN SOUTHEAST ASIA

Ali Fatehi and Keith D. Koper

Saint Louis University

Sponsored by the Air Force Research Laboratory

Contract No. FA8718-06-C-0003

ABSTRACT

We have used data from the small aperture Chiang Mai seismic array (CMAR) in Thailand to characterize P-wave propagation in the mantle transition zone beneath south Asia. Our data consist of nearly 1700 events, which occurred at regional distances from CMAR with continental ray paths. We used time domain beam-forming techniques to estimate the 2D slowness vectors of all the first arriving energy and found only mild anomalies in back azimuth from what is predicted for the U.S. Geological Survey (USGS) epicenters. We also found that later arriving energy, appearing either as discrete secondary phases or as part of the coda, arrives along the great circle paths as well. This justified the use of slant-stack techniques that assume great circle propagation but retain high resolution in time. We designed an algorithm that generates smoothed slant-stacks and automatically picks local maxima in time-ray parameter space for a user-defined level of significance. The resulting values were averaged into time-distance bins in order to generate an image of P wave propagation across the region. We find that when large numbers of data are combined, the resulting images tend to be smeared and lack clear signals from triplications associated with the 410-km and 660-km discontinuities. This is true for a variety of frequency bands, beam formation techniques, binning parameters, and alignment techniques. In general, differences among source properties and lateral variation in Earth structure are significant enough to defocus the images. However, we find that triplicated arrivals are often visible for individual events and small geographical clusters of events.

We have implemented a modeling technique that uses a niching genetic algorithm to globally search the model space and find groups of acceptable models. The models are described by 10–12 parameters that represent P velocities at nodes in the upper mantle, as well as the depths for discontinuities near 410 km and 660 km. We have experimented with objective functions defined using the curvature of the first arriving travel time curve, differential travel times at various distances, and combinations of the two. Estimates of differential ray parameters for multiple arrivals are not included in the objective function because the predicted differences are generally too small to be observed robustly at CMAR. Tests with noise-free synthetic data indicate good recovery of the input model in the upper mantle, with discontinuity depths usually within ±5 km, and velocity jumps within 20%. We are currently working on developing 1D models for the individual events and event groupings in which triplicated arrivals are confidently observed.

OBJECTIVES

Detection and location of small magnitude seismic events is one the current challenges of verification seismology. Local and regional analysis of small magnitude data is of great importance since these data do not produce sufficient teleseismic data. Locally recorded phases such as Pn, Pg, and Lg, show considerable variability in travel time and waveform character from region to region, since they travel in the lithosphere, which is the most heterogeneous layer of the Earth. Regional P waveforms are also complicated since they turn in the mantle transition zone (MTZ). The two global discontinuities at 410 and 660 km depth that bound the MTZ, cause the multipathing of P waves in which several distinctive P waves arrive in a short time window. Although the MTZ is less heterogeneous than the lithosphere, it has significant lateral variations, which makes the situation even more complicated. Two other seismic discontinuities are also thought to exist at least in specific regions at depths near 220 km (Gu et al., 2001) and 520 km (Shearer, 1996; Ryberg et al., 1997).

It is important to understand regional distance P-wave propagation in verification studies. Multipathing can reduce the amplitude of the first arriving P wave by partitioning energy into later arriving phases. This effect should be recognized and accounted for to avoid underestimating the magnitude of the seismic event. Multipathing can also bias the observation of depth phases. Depth phases from the crustal events can arrive in the same time window as later arriving waves from the MTZ. Due to the importance of event depth as a discrimination factor, it is crucial to distinguish between wave types.

The goals of this study are to document and model P wave multipathing owing to discontinuities and velocity gradients in the upper mantle beneath south Asia. We use data from the CMAR array in Thailand, which occurred between 1/1/1995 and 12/31/2005. The events have epicentral distances of 13°–30° with primarily continental paths. We use array-processing techniques to determine the subtle differences in arrival time and slowness of multipathed P waves. First arrival and differential time (later-arriving relative to first arrival) data are used to generate 1D velocity models for specific geographic corridors.

RESEARCH ACCOMPLISHED

Development of the CMAR Database

The relevant CMAR data used in this study consist of about 1700 events with magnitude of at least 4.0 mb, that occurred in South Asia at distances of 13^{o}–30^{o} from the CMAR. At these distances waves turn in the upper mantle and have potentially complicated interactions with discontinuities and velocity gradients in the transition zone. We selected events that provided continental paths to the CMAR and for which P-wave arrival times had been reported to the USGS. The seismicity covers a wide range of distances and azimuths yielding ray paths that preferentially sample the complicated tectonics of the India-Eurasia collision zone (Figure 1). Nearly all of the events are at shallow depths, though a significant group of intermediate depth events occur in the Hindu-Kush region at distances of 25^{o}–30^{o} from CMAR.

Array Processing of CMAR Data

The Chiang Mai Array (CMAR) is deployed in northern Thailand and consists of 18 short-period, vertical-component seismometers deployed with an effective aperture of about 10 km. The station geometry leads to an array response function that is roughly symmetrical but also relatively broad. At 1 Hz the side lobes of the array response function are outside of the relevant slowness domain; however the main peak has a half-width of about 4 s/deg. The relatively low precision of the array makes it challenging to discriminate among triplicated arrivals based on ray parameter, since multiply arriving waves are often predicted to have differential slownesses on the order of 0.5–2.0 s/deg.

Using seismic array techniques has two primary advantages: an increase in signal-to-noise ratio and the ability to robustly determine the direction from which seismic energy arrives. We used the Generic Array Processing (GAP) software package (Koper, 2005) for the array processing of CMAR data. In GAP slowness analysis is done in the time domain by repeated beam formation over a grid of potential slowness vectors. A variety of beam-forming techniques are available such as simple delay and sum, nth root stacking, and phase-weighted stacking (PSW) (Rost and Thomas, 2002). The non-linear beamforming techniques (i.e., PSW) often lead to a much higher increase in signal-to-noise compared to the $\sqrt{N}$ enhancement expected from linear approaches.

Within GAP Cartesian or polar components of the 2D horizontal slowness vector can be obtained simultaneously. Ray parameter and back azimuth can be inferred while one of them is held constant. There is also the capability of inferring the relative slowness between two phases or time windows. In all cases uncertainties for slowness parameters are determined with a stochastic bootstrap-type error estimation algorithm (i.e., Tichelaar and Ruff, 1989). For example, when estimating uncertainties associated with the estimate of a horizontal slowness vector, a pseudo-array is generated by randomly resampling the N array traces with replacement until N traces have been selected. A grid search is then carried out on the pseudo-array to determine the optimal slowness vector. This process is repeated M times to generate a population of optimal slowness vectors. This population is then used to calculate the model covariance matrix, from which a 95% confidence ellipse can be determined. Alternatively, error bounds on either the ray parameter or back azimuth can be estimated from the population of bootstrap solutions.

Figure 2 shows the PSW slant-stack (bottom left) and the optimal 2D slowness vector search (bottom right) for a mb = 6.1 event at a distance of 24.7° from the CMAR. This event was a nuclear test that occurred at Lop Nor, China on May 15, 1995. Beam amplitude is calculated using a 3rd-order phase-weighted stack (PSW) that significantly amplifies coherent energy while providing less waveform distortion than N-th root stacking (Schimmel and Paulssen, 1997). A record section of the waveforms for this event is also shown in the figure (top left). The slant-stack has been obtained using a fixed back azimuth of 335°. At this distance transition zone multipathing can be expected. The result of slant-stack shows a few later arrivals from which the first one arrives about 10 s after the primary P wave. For this later arriving phase, a grid search could be carried out to obtain the optimal differential ray parameter.

Slowness Residuals and Slowness-Azimuth Station Corrections (SASC)

We have obtained slowness residuals of the first P wave arrivals for all the events with quality data. For each event, the reported depth and distance in the USGS preliminary determination of epicenters (PDE) catalog have been used to compute the theoretical 2D slownesses, assuming propagation in IASPEI91. We used these slowness residuals to obtain SASC corrections for the CMAR. The SASC map (Figure 3, left) is produced using the method explained by Bondar et al. (1999). Events with mb ≥ 4.7 and bins with the minimum of two observations were used in computing the corrections. When data permits, it is ideal to set the number of minimum observations to higher values. Figure 3 (right) shows the same corrections obtained by Bondar et al. (1999) for the CMAR using a different data set. Our residuals show a consistent azimuthal bias, which is likely due to heterogeneous structure beneath the CMAR, such as a dipping Moho. The mean of the back azimuth residuals however, is small enough to justify using a fixed back azimuth, slant-stack (or vespagram) approach.

Vespagram Stacking

To obtain a coherent picture of later-arriving phases we stacked the vespagrams of the events and binned the results in time and distance. This gives the hit count, or a 2D histogram of number of arrivals in time and distance. To identify the later arrivals in slant-stacks, we used an automated algorithm to pick the arrival time and ray parameter of all local maxima whose beam amplitude is above a given threshold. The threshold value is a fraction of the global maximum value of the beam amplitude for each event. Due to the presence of other arrivals (depth phases and scattered energy) we did not get a coherent travel time curve from the stacking of the vespagrams. To eliminate some of the spurious arrivals, we smoothed the slant-stacks prior to arrival picking. Smoothing reduces some of the noise by averaging the data and eliminating some of the local minima in slant-stacks.

Figure 4 (top) shows the smoothed version of a slant-stack for an event (mb = 4.6, Δ = 26.38°) in which the black circles show the arrivals, which were picked automatically using a fraction value of 0.5. Arrival picking from the smoothed slant-stacks provides better results but the problem of unwanted arrivals still exists. For instance, unless we are able to identify the depth phases, the automatic picker will pick them, if they have higher amplitude than the threshold value. Figure 4 (bottom left) shows the 2D histogram (hit counts) of the arrivals (picked from the smoothed slant-stacks using a fraction value of 0.5) for all events using a bin size of 1° × 1 s. The bottom right figure shows the binned results for ray parameter vectors of the same arrivals. Vectors shown in the figure are the average of the vectors in each bin. In both figures the preliminary reference Earth model (PREM) travel time curve is shown for comparison.

Incoherent Stacking of Array Beams

We produced an event stack of receiver beams to reduce some of the noise in the beams of closely located events. This method works better if one is able to stack events in smaller distance bins. We binned the events in 1° bins and produced the stack of the beams in each bin. Stacks were computed relative to the theoretical first arrival and to the manually picked first arrival of each beam. While some of the beam stacks showed a little improvement in noise reduction, we did not observe a consistent pattern of later arriving phases in our final stacks. Since our data covers a wide range of back azimuths (Figure 1), we formed 2D bins of data (1° distance and 10° back azimuth) and computed the stack of the beams in each bin. Stacks in some bins show later arrivals consistent with those predicted by PREM or IASPEI91. In general the two methods of imaging later arrivals (vespagram and beam tacking) show effectiveness in certain geographic corridors but not over the entire region.

Modeling Observed First Arrivals

First P-wave arrival times, which have been manually picked for 2D slowness analysis, were used for modeling the Earth structure (including MTZ) in our study region. Among the 1700 events, 1562 events had a readable first arrival. We binned the data in distance and used the mean and standard deviation of each bin in modeling. To reduce the effect of depth on first arrivals we shifted the binned data by their mean: each mean (in a specific bin) is considered a data point. We took the mean of all data points and subtracted it from each data point. The results are our final observed first arrivals to be modeled. In this way we do not model the absolute travel times but mostly the shape of the travel time curve (Figure 5, left).

Uppermost mantle and MTZ structure affect the shape of the travel time curve at regional distances. Figure 5 (right) shows the effect of a change in MTZ alone on travel time curve. We modeled the first arrival data allowing the variation only in MTZ structure. We then extended our method to include crust and upper mantle structures in the modeling using a niching genetic algorithm (NGA) (Koper et al., 1999). Several tests were done using synthetic data to fine-tune the NGA input parameters, which helps to decide on appropriate model parameters. Observed first arrivals were binned (0.4° bin size) and both observed and theoretical data were shifted as explained earlier. A least-squares approach was used in defining the misfit between the observed and theoretical data and the standard deviations of the observed data in each bin were used as weighting factors. The set of acceptable Earth models broadly spans the search bounds, as the first arrivals provide a relatively soft constraint on structure; however this constraint can be valuable when combined with observations of later arrivals.

Modeling Later Arriving and Differential Times

Figures 4 (bottom left) shows the results of stacking smoothed versions of vespagrams. Because of the presence of other arrivals it is not easy to model the stacks. It is also not feasible to identify other phases and eliminate them from the stacks. Besides these problems, location errors also introduce bias in the stacking results when we compare them to the theoretical data. For these reasons we computed differential times for each event from the individual slant-stacks and then stacked the results in time and distance. Differential time stacks are also contaminated by other arrivals and may not be easy to model. Because of this decoherence in the stacks we intend to model individual beams, and small groups of beams, in which triplicated phases can be confidently observed. So far we have performed synthetic tests that indicate recovery of test models is feasible if enough observations are used (Figure 6).

CONCLUSIONS AND RECOMMENDATIONS

The small aperture of the CMAR makes it challenging to identify triplicated P waves on the basis of differential ray parameters. We have tried a variety of binning, stacking, and beam-forming techniques, but it is difficult to produce coherent images of upper mantle triplications when combining beams from many different events. In general, the differences in source properties and lateral variations in Earth structure are large enough to trump the expected signal from waves interacting with transition zone discontinuities. However, for many individual events and small groups of events, it is possible to detect the expected signal. For these cases we have a developed a non-linear global search technique that finds groups of acceptable radial Earth models. Tests with synthetic data indicate that features such as the depths and velocity changes associated with transition zone discontinuities are reasonably well-resolved when a large enough number of later-arriving phases are included. We are currently applying this modeling technique to the data in which we the have the most confidence in the coherence of later arriving phases.

REFERENCES

Bondar, I., R. G. North, and G. Beall (1999). Teleseismic slowness-azimuth station corrections for the International Monitoring System seismic network, *Bull. Seism. Soc. Am*. 89: 989–1003.

Gu, Yu. J., A. M. Dziewonski, and G. Ekstrom (2001). Preferential detection of the Lehman discontinuity beneath continents, *Geophys. Res. Lett*. 28: 4655–658.

Koper, K .D. (2005). The Generic Array Processing (GAP) software package, Annual SSA Meeting, Lake Tahoe, NV.

Koper, K. D., M. E. Wysession, and D. A. Wiens (1999). Multimodal function optimization with a niching genetic algorithm: A seismological example, *Bull. Seism. Soc. Am*. 89: 978–988.

Rost, S. and Ch. Thomas (2002). Array seismology: Methods and applications, *Rev. of Geophys*. 40: 1008, doi:10.1029/2000RG000100.

Ryberg, T., F. Wenzel, A. V. Egorkin, and L. Solodilov (1997). Short-period observation of the 520 km discontinuity in northern Eurasia, *J. Geophys. Res*. 102: 5413–5422.

Schimmel, M. and H. Paulssen (1997). Noise reduction and detection of weak, coherent signals through phase weighted stacks, *Geophys. J. Int*. 130: 497–505.

Shearer, P. M. (1996). Transition zone velocity gradients and the 520-km discontinuity, *J. Geophys. Res*. 101: 3053–3066.

Tichelaar, B. W. and L. J. Ruff (1989). How good are our best models? Jacknifing, bootstrapping, and earthquake depth, *Eos Trans. AGU*, 70.

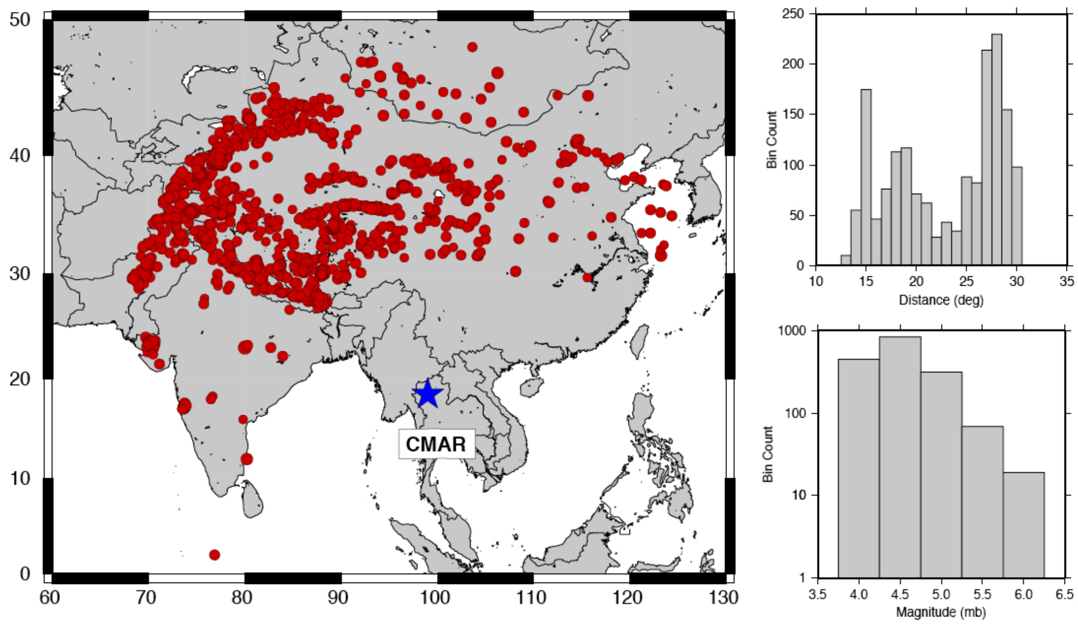

Figure 1. (Left) Epicenters for nearly 1700 seismic events that occurred at distances of 13°–30° from the CMAR from Jan. 1995 through Oct. 2005. Only events with primarily continental paths to the CMAR and mb ≥ 4.0 were selected. (Right) histograms of epicentral distance (top) and magnitude of the events.

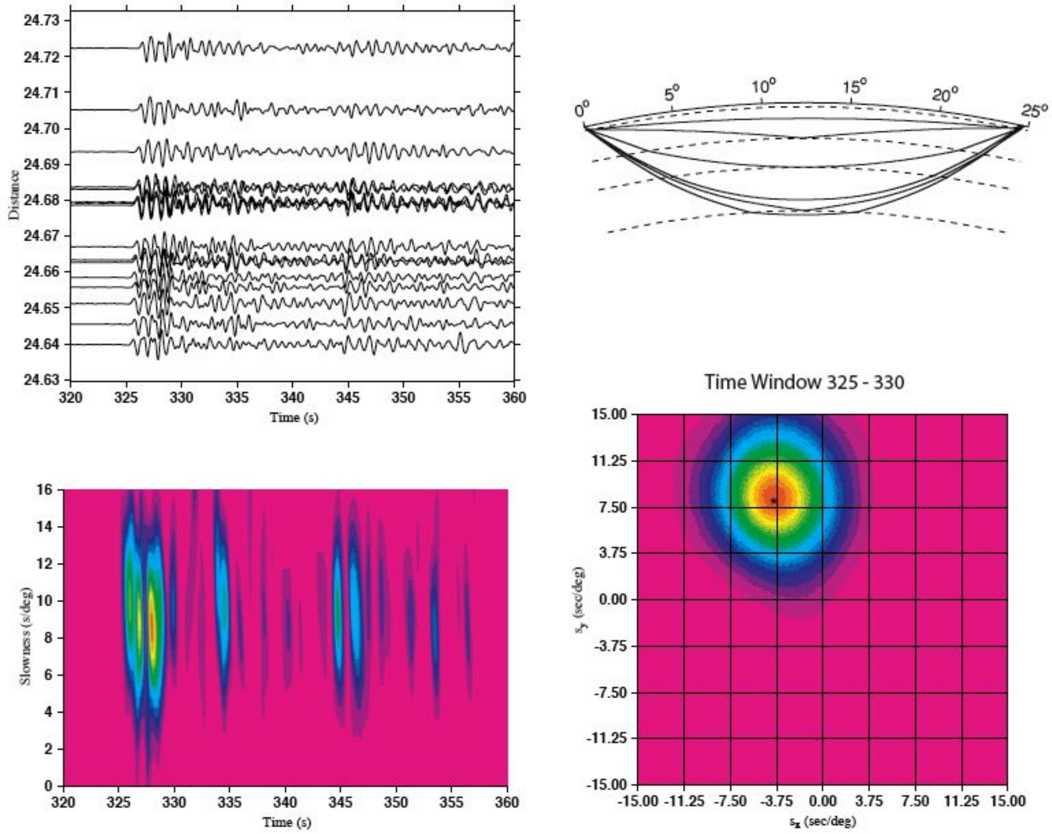

Figure 2. (Top left) Record section of waveforms for a mb = 5.0 event with a epicentral distance of 27.7°. (Top right) PSW slant-stack of the event assuming a fixed back azimuth of 311°. (Bottom) Grid search results for the optimal 2D slowness vector in the time window of the first P wave.

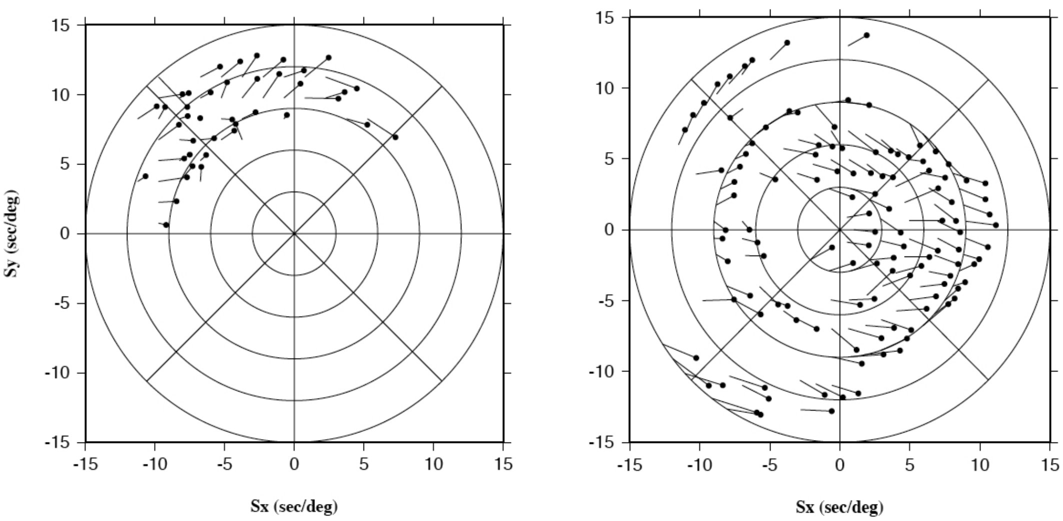

Figure 3. (Left) Slowness-azimuth station correction for CMAR obtained from the binned slowness residuals of first arrivals. The average residuals in each bin are shown as vectors in which the base of the vectors are the observed values and the circles are the theoretical values. Only events with mb ≥ 4.7 and bins with at least 2 observations are used. (Right) Same corrections for CMAR obtained by Bondar et al. (1999) using a different data set.

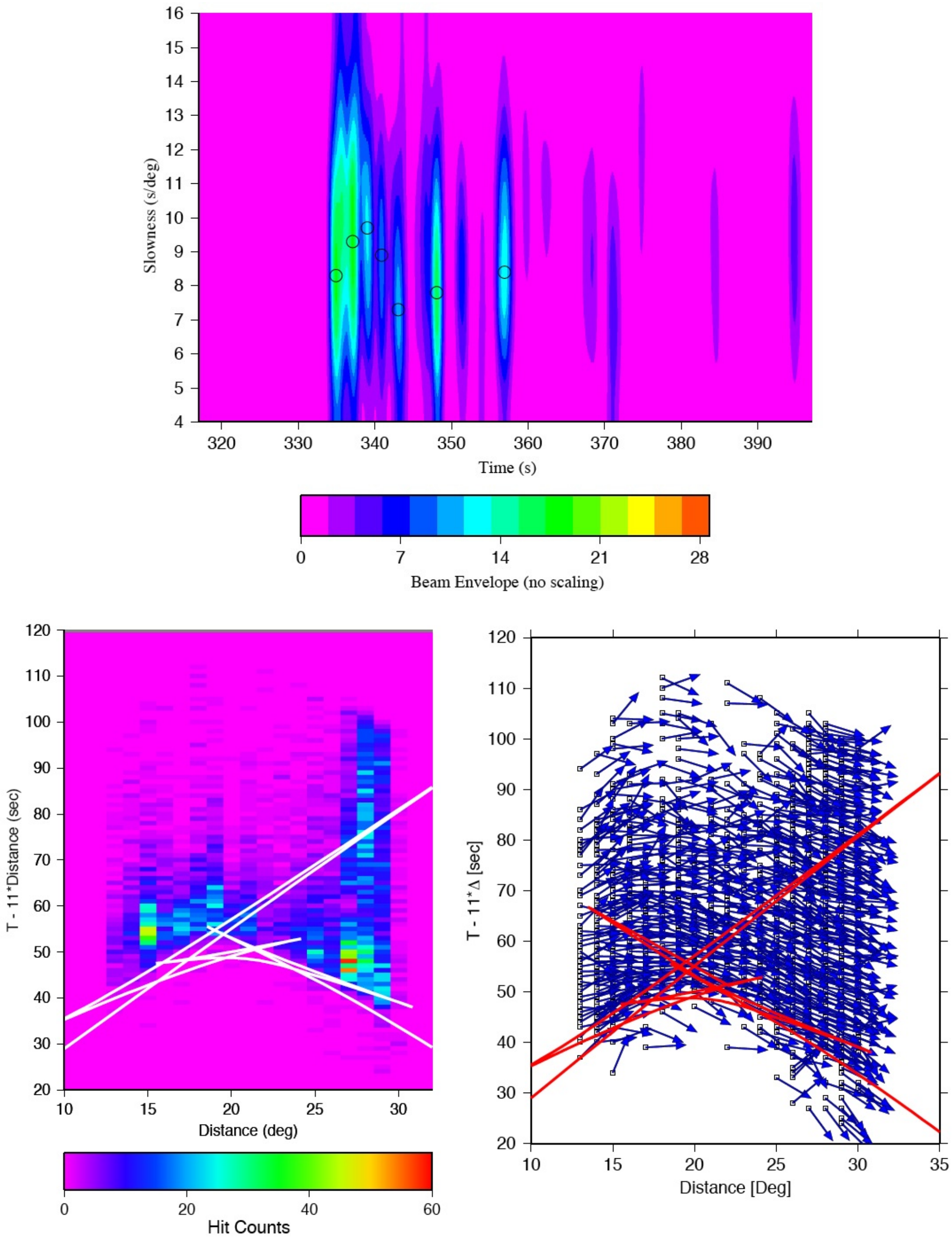

Figure 4. (Top) Smoothed version of the slant-stack for an event with mb = 4 .6 and Δ = 2 6.38°. Black circles show the arrivals picked by an automatic picker using a fraction value of 0.5. (Bottom left) 2D histogram of the arrivals for all events with quality data (picked as shown in top figure) binned by 1° $\times$ 1 s. (Right) binned results for the (bin average) ray parameter vectors obtained from the smoothed slant-stacks of the events. PREM travel time curve is shown in both (bottom) figures for comparison.

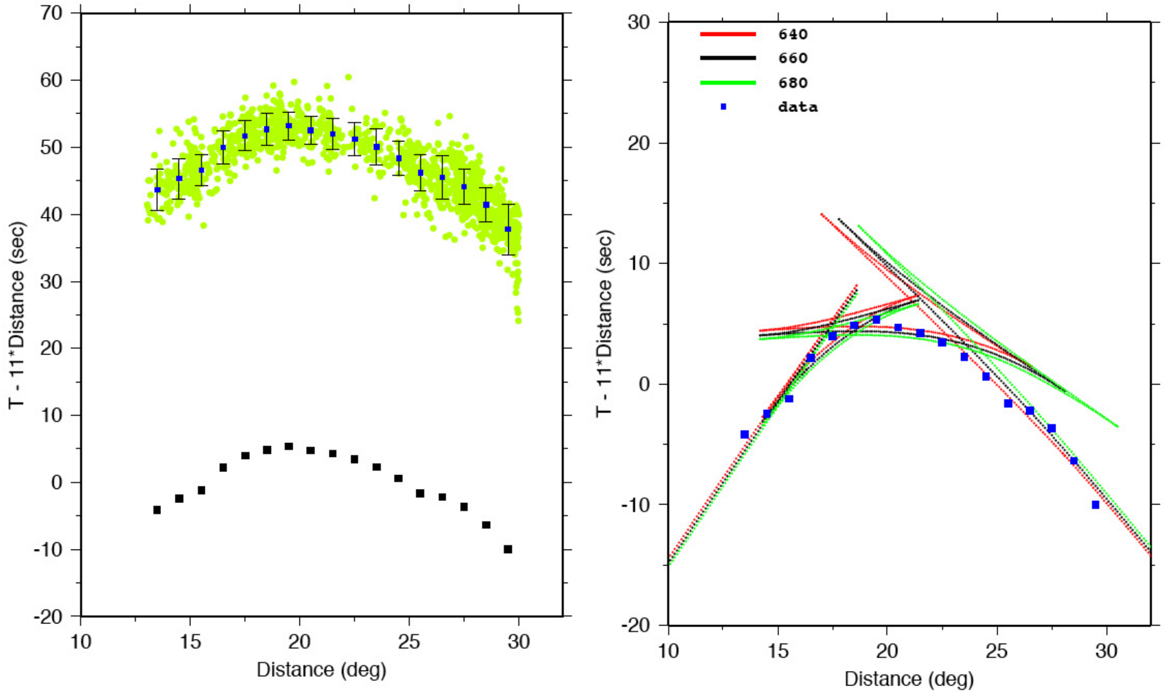

Figure 5. (Left) Manually picked arrival times (green circles) for 1562 events are binned using a bin size of 1°. Blue squares and error bars represent the mean and standard deviation in each bin. Black squares show the shifted data to be used in modeling (see text for explanation). (Right) Changes in travel time shape for different models. Data (binned in 1° bins) and models are shown after shifting. Only the 660 depth has been changed in the models.

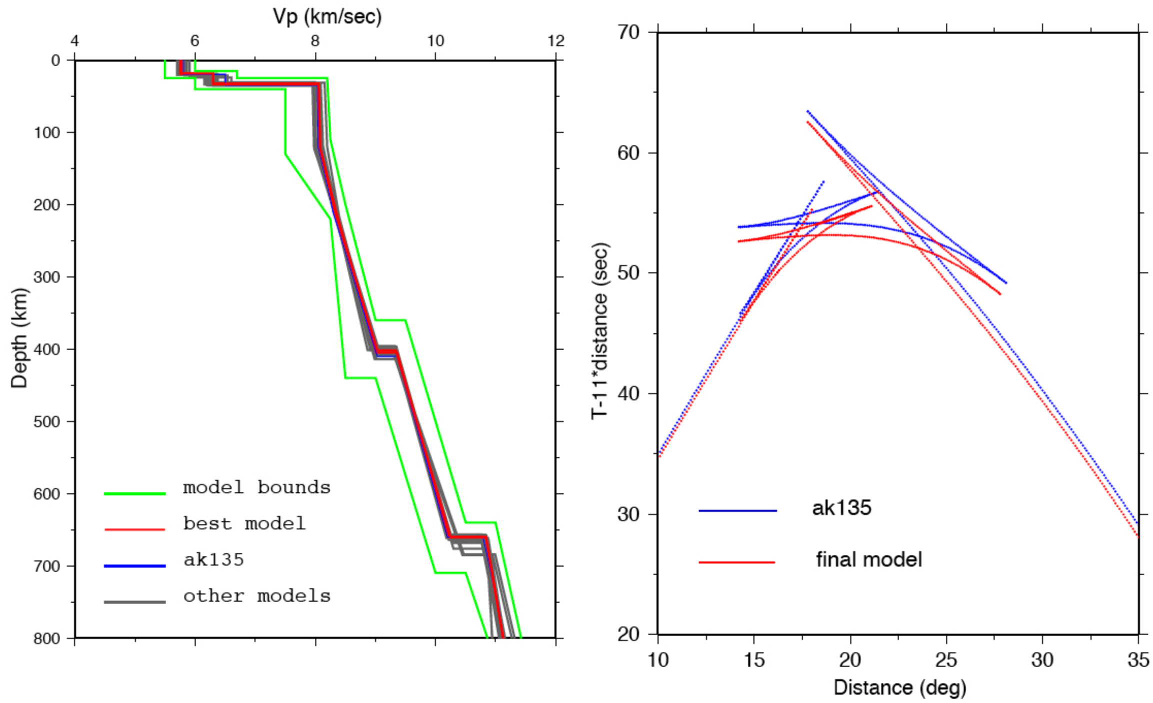

Figure 6. (Left) Velocity models obtained from the modeling of synthetic differential times (later arriving relative to first arrival) using NGA. The 410 discontinuity depth in the best model was 405 km. Except for crustal structure and 410 depth all other parts of the velocity model (by which the synthetics were created) were obtained from the modeling with insignificant differences.